

Moments of singlet parton densities on the lattice in the Schrödinger Functional scheme

Filippo Palombi^a, Roberto Petronzio^a, Andrea Shindler^{a,b}

^a*Dipartimento di Fisica, Università di Roma Tor Vergata*

and INFN, Sezione di RomaII,

Via della Ricerca Scientifica 1, 00133 Rome, Italy

^b*Deutsches Elektronen-Synchrotron, DESY*

Platanenallee 6, D-15798 Zuthen, Germany

Abstract

A non perturbative computation of the evolution of singlet parton densities without gauge-fixing requires a gauge invariant gluon source operator. Within the Schrödinger Functional scheme (SF), such a source can be defined in terms of path ordered products of gauge links, connected to the time boundaries. In this paper we adopt this definition and perform a one loop lattice computation of the renormalization constants of the twist-2 operators that correspond to the second moment of singlet parton densities. This calculation fixes the connection between the lattice SF scheme where a non perturbative evaluation of the absolute normalization of singlet parton densities can be made at low energy and the \overline{MS} scheme where one can extract the experimental values.

Keywords: lattice QCD, perturbation theory, structure functions.

1. Introduction

Non perturbative calculations of parton densities are the only possibility to fix their absolute normalization from first principles. Lattice simulations are suitable to this purpose and various estimates have been presented in the literature for the first moments of valence quark densities [1,2,3,4]. In general, experimental values of moments of the structure functions are obtained by comparing production rates with theoretical cross sections in common continuum scheme at high energy, where perturbation theory becomes reliable. For the non singlet case, the matching of low energy estimates of hadron matrix elements of Wilson operators in lattice schemes with their experimental values has been realized within the Schrödinger Functional scheme (SF), integrated by a finite size recursive method to match the large gap of the energy scales involved. A crucial element of the calculation was the non perturbative evolution of the Wilson operator taken in a matrix element with a proper SF quark *source* that defined the SF scheme [5]. An analogous calculation for the gluon density and in general for the singlet parton densities involving the mixing between gluon and sea quark densities has not yet been attempted, given the difficulties in accounting the sea quark pair creation through unquenched simulation algorithms. In this paper we propose a definition in the SF scheme of a gluon source that can be used to evaluate the non perturbative running of the mixing renormalization matrix characterising the singlet evolution. Using the Wilson action and the Feynman gauge, we perform a one loop calculation that fixes the relation between the SF singlet scheme and the \overline{MS} scheme for the second moment of singlet densities. Such a calculation is preliminary to the non perturbative evaluation of the singlet densities hadron matrix elements and to their comparison with experimental data. The method can be extended to higher moments where the experimental information is scarce [6] and even a modest precision can help fixing the gluon density at momentum fraction greater than 0.5 [7].

The paper is organized as follows: section 2 contains basic definitions of the SF scheme, singlet operators and SF quark source. In section 3 a gauge invariant gluon source is introduced and its perturbative $O(g_0^2)$ expansion is performed. In section 4 we define correlation functions involving singlet operators, perform the one loop calculation and in section 5 we extract the one

loop renormalization constants of the singlet operators.

2. Singlet Structure Functions

2.1 Schrödinger Functional

This section is only meant to recall some basic facts that have been discussed exhaustively in the literature [8]. The theory is set up on a hyper-cubic euclidean lattice with spacing a and size $T \times L^3$ (throughout the paper we put $T = L$, writing T whenever it has to be recalled the time character of the variable). The Schrödinger functional represents the amplitude for the time evolution that takes into account quantum fluctuations of a classical field configuration between two predetermined classical states. It takes the form of a standard functional integral with fixed boundary conditions. Explicitly, the link variables are chosen to be periodic in space and to satisfy Dirichlet boundary conditions in time,

$$A_k(x)|_{x_0=0} = C(\mathbf{x}), \quad A_k(x)|_{x_0=T} = [\mathbb{P}C'](\mathbf{x}), \quad (2.1)$$

where $C(\mathbf{x})$ and $C'(\mathbf{x})$ are fixed boundary fields, and \mathbb{P} projects onto the gauge invariant content of $C'(\mathbf{x})$ [8]. Here we choose $C = C' = 0$, leading to the boundary conditions

$$U(x, k)|_{x_0=0} = \mathbb{I}, \quad U(x, k)|_{x_0=T} = \mathbb{I}; \quad k = 1, 2, 3 \quad (2.2)$$

for the lattice gauge field. The only gauge transformations on the boundary time slices that preserve such boundary conditions are the global ones [8]. This property will be crucial for the definition of the gauge invariant surface sources. The quark fields are chosen to be periodic up to a phase in the three space directions,

$$\psi(x + L\hat{k}) = e^{i\theta_k} \psi(x), \quad \bar{\psi}(x + L\hat{k}) = \bar{\psi}(x) e^{-i\theta_k}; \quad k = 1, 2, 3 \quad (2.3)$$

where θ_k is kept as a free parameter. One can also distribute the phase to all lattice points by an abelian transformation on the Fermi fields, i.e. by changing the form of the usual lattice

derivative in

$$\nabla_\mu \psi(x) = \frac{1}{a} [\lambda_\mu U(x, \mu) \psi(x + a\hat{\mu}) - \psi(x)] \quad (2.4)$$

$$\nabla_\mu^* \psi(x) = \frac{1}{a} [\psi(x) - \lambda_\mu^{-1} U(x - a\hat{\mu}, \mu)^{-1} \psi(x - a\hat{\mu})] \quad (2.5)$$

where

$$\lambda_\mu = e^{ia\theta_\mu/L}; \quad \theta_0 = 0, \quad -\pi < \theta_k \leq \pi \quad (2.6)$$

It is useful to define also the backward derivatives on the lattice

$$\bar{\psi}(x) \overleftarrow{\nabla}_\mu = \frac{1}{a} [\bar{\psi}(x + a\hat{\mu}) U(x, \mu)^{-1} \lambda_\mu^{-1} - \bar{\psi}(x)] \quad (2.7)$$

$$\bar{\psi}(x) \overleftarrow{\nabla}_\mu^* = \frac{1}{a} [\bar{\psi}(x) - \bar{\psi}(x - a\hat{\mu}) U(x - a\hat{\mu}, \mu) \lambda_\mu] \quad (2.8)$$

Similarly to the gauge field, Dirichlet boundary conditions are imposed on the quark fields,

$$P_+ \psi(x)|_{x_0=0} = \rho(\mathbf{x}), \quad P_- \psi(x)|_{x_0=T} = \rho'(\mathbf{x}), \quad (2.9)$$

and

$$\bar{\psi}(x) P_-|_{x_0=0} = \bar{\rho}(\mathbf{x}), \quad \bar{\psi}(x) P_+|_{x_0=T} = \bar{\rho}'(\mathbf{x}), \quad (2.10)$$

The Schrödinger functional action, including Feynman rules for the fermionic part and further details can be found in [8,9].

2.2 Singlet operators

In the continuum, moments of singlet structure functions are related, through the operator product expansion, to hadronic matrix elements of two kind of twist-2, gauge invariant, local operators of the form

$$\begin{aligned}
O_{\mu_1 \dots \mu_N}^q &= \frac{1}{2^N} \bar{\psi} \gamma_{[\mu_1} \overleftrightarrow{D}_{\mu_2} \dots \overleftrightarrow{D}_{\mu_N]} \psi \\
O_{\mu_1 \dots \mu_N}^g &= \sum_{\rho} \text{tr} \{ F_{[\mu \rho} \overleftrightarrow{D}_{\mu_2} \dots \overleftrightarrow{D}_{\mu_{N-1}} F_{\rho \mu_N]} \}
\end{aligned} \tag{2.11}$$

where brackets $[\dots]$ mean Lorentz indices symmetrization and $\overleftrightarrow{D}_{\mu} = \overrightarrow{D}_{\mu} - \overleftarrow{D}_{\mu}$, with

$$\overrightarrow{D}_{\mu} = \frac{1}{2}(\nabla_{\mu} + \nabla_{\mu}^*), \quad \overleftarrow{D}_{\mu} = \frac{1}{2}(\overleftarrow{\nabla}_{\mu} + \overleftarrow{\nabla}_{\mu}^*) \tag{2.12}$$

The operators in eq. (2.11) belong in the continuum to irreducible representations of the angular momentum. On the lattice, given the lower (hypercubic) symmetry of the Euclidean lattice action with respect to that of the continuum (all 4-d rotations), the identification of an irreducible representation may require some particular combination of operators. This classification has been discussed for example in refs. [10,11]. A subset of the basis described in [11], involving only spatial indices is given by

$$O_{12}^q(x) = \frac{1}{4} \bar{\psi}(x) \gamma_{[1} \overleftrightarrow{D}_{2]} \psi(x) \tag{2.13}$$

$$O_{12}^g = \sum_{\rho} \text{tr} \{ F_{[1\rho}(x) F_{\rho 2]}(x) \} \tag{2.14}$$

and

$$F_{\mu\nu}(x) = \frac{1}{8a^2 g_0} \{ Q_{\mu\nu}(x) - Q_{\nu\mu}(x) \} \tag{2.15}$$

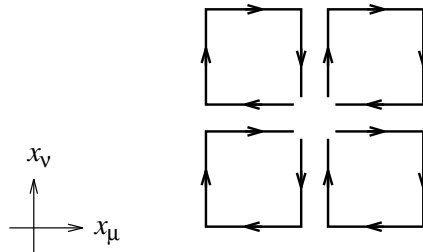


Fig. 1. Graphical representation of the products of gauge field variables contributing to the lattice field tensor, eq. (2.15). The point x is at the center of the diagram where all loops start and end.

with $Q_{\mu\nu}(x)$ being the sum of the plaquette loops shown in Fig. 1, maximizing the symmetry of the field strength on the lattice. The usual plaquette representation of the field strength transforms like a reducible representation of the hypercubic group, while the definition *clover*-like of eq. (2.15) transforms like an irreducible one.

The correlation functions we want to study can be organized in a 2×2 matrix as follows

$$f_{\alpha\beta} \sim \begin{bmatrix} \langle \mathcal{O}_q \mathbb{S}_q \rangle & \langle \mathcal{O}_q \mathbb{S}_g \rangle \\ \langle \mathcal{O}_g \mathbb{S}_q \rangle & \langle \mathcal{O}_g \mathbb{S}_g \rangle \end{bmatrix} \quad (2.16)$$

where \mathcal{O} 's are the operators and \mathbb{S} 's are the quark and gluon sources, defined in the following sections. Beyond the tree-level there will be in general a mixing in the flavor singlet sector between the quark operator (2.13) and the gluon operator (2.14). However in the *quenched* approximation ($N_f = 0$) one has $\langle \mathcal{O}_{\mu\nu}^q \mathbb{S}_g \rangle = 0$. In this case the matrix (2.16) becomes triangular and the operator \mathcal{O}^q does not mix with \mathcal{O}^g .

2.3 Fermionic source

To probe operators (2.13) and (2.14) in correlation functions, one must choose suitable sources. In the case of the quark source we make the same choice of the non singlet calculation [13]. As already stressed in that paper, the SF scheme allows us to define a gauge invariant source that provides a spatial direction. The operator (2.13) needs two directions and we have to give to the quark state a momentum different from zero in one extra direction. Moreover, using a particular feature of the SF, we can use the constant phase term θ defined in (2.3), called a *finite-size* momentum. The reason for this name is that, at finite volume, this phase acts like a momentum probed by the local operators that we want to renormalize, but unlike the standard lattice momentum, it escapes the quantization rule induced by the finite volume. Its value can be chosen smaller than the minimum value of the standard momentum $p_{min} = \frac{2\pi}{L}$, reducing the associated important lattice artefacts [13]. The quark bilinear at the boundary is given by the expression

$$\mathbb{S}_q(\mathbf{p}) = a^6 \sum_{\mathbf{y}, \mathbf{z}} e^{i\mathbf{p} \cdot (\mathbf{y} - \mathbf{z})} \bar{\zeta}(\mathbf{y}) \gamma_2 \zeta(\mathbf{z}) \quad (2.17)$$

3. Gauge invariant gluon source

In this section we introduce a gauge invariant gluon source which can be used for the calculation of the singlet correlation functions [12]. To exploit the features of the SF we recall that the gauge group of the SF is local in the bulk and global on the boundaries. This makes the quark source (2.17) gauge invariant. The gauge invariant gluon source is defined by

$$\mathbb{S}_g = \mathcal{S} = \text{tr}\{\mathcal{T}_1 \mathcal{T}_2\} \quad (3.1)$$

where the trace is over the color indices. The *big-tooth* state \mathcal{T}_i is defined by

$$\mathcal{T}_i = \frac{a^3}{2i} \sum_{\mathbf{x}} \left\{ \Pi_i(\mathbf{x}) - \Pi_i^\dagger(\mathbf{x}) \right\} \quad (3.2)$$

and

$$\Pi_i(\mathbf{x}) = \frac{1}{ag_0} \prod_{x_0=0}^{\frac{T}{4}-a} U_0(x_0, \mathbf{x}) U_i\left(\frac{T}{4}, \mathbf{x}\right) \prod_{x_0=\frac{T}{4}-a}^0 U_0^{-1}(x_0, \mathbf{x} + a\hat{i}) \quad (3.3)$$

It is natural to define a gluon source also associated with the boundary $x_0 = T$.

$$\mathcal{S}' = \text{tr}\{\mathcal{T}'_1 \mathcal{T}'_2\} \quad (3.4)$$

$$\mathcal{T}'_i = \frac{a^3}{2i} \sum_{\mathbf{x}} \left\{ \Pi'_i(\mathbf{x}) - \Pi'^{\dagger}_i(\mathbf{x}) \right\} \quad (3.5)$$

$$\Pi'_i(\mathbf{x}) = \frac{1}{ag_0} \prod_{x_0=T-a}^{\frac{3}{4}T} U_0(x_0, \mathbf{x}) U_i\left(\frac{3}{4}T, \mathbf{x}\right) \prod_{x_0=\frac{3}{4}T}^{T-a} U_0^{-1}(x_0, \mathbf{x} + a\hat{i}) \quad (3.6)$$

Eq. (3.4) is necessary in order to define the correlation function which will be used to remove the additional divergences of the singlet correlation functions, introduced by the source. A graphical representation of the source is reported in Fig. 2. It is a product of temporal links in the time direction from $x_0 = 0$ to $x_0 = T/4$, connected with a spatial link, or from $x_0 = T$ to $x_0 = 3T/4$. It is gauge invariant, has two spatial directions (the same ones of the operators

(2.13) and (2.14)), and is projected at zero momentum. The gluon source at $x_0 = T$ cannot be obtained by substituting in \mathcal{S} $x_0 = T/4$ with $x_0 = 3T/4$. The source gives rise to linear and logarithmic divergences: our calculation in perturbation theory shows that they are removed by a proper normalization of the correlation functions where it appears.

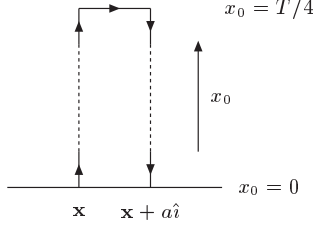


Fig. 2. Graphical representation of $\Pi_i(\mathbf{x})$.

3.1 Perturbative expansion of the gluon source

The perturbative expansion of the gluon source is straightforward. In the SF we adopt as usual the time-momentum scheme defined in [9]. For the color matrices we follow the same convention of [9]. So we have

$$U(x, \mu) = \exp\{ag_0 q_\mu^a(x) T^a\} \quad (3.7)$$

$$q_0^a(x) = \frac{1}{L^3} \sum_{\mathbf{p}} e^{i\mathbf{p} \cdot \mathbf{x}} \tilde{q}_0^a(x_0; \mathbf{p}) \quad (3.8)$$

$$q_k^a(x) = \frac{1}{L^3} \sum_{\mathbf{p}} e^{i\mathbf{p} \cdot \mathbf{x}} e^{\frac{i}{2} a p_k} \tilde{q}_k^a(x_0; \mathbf{p}) \quad (3.9)$$

The sum over the momenta \mathbf{p} runs in the range $-\pi/a < p_k \leq \pi/a$ with

$$\mathbf{p} = (p_1, p_2, p_3), \quad p_k = \frac{2\pi}{L} n_k, \quad n_k \in \mathbb{Z} \quad (3.10)$$

The Feynman rules associated with the gluon sources are found expanding in powers of g_0

$$\mathcal{T}_i = \mathcal{T}_i^{(0)} + g_0 \mathcal{T}_i^{(1)} + g_0^2 \mathcal{T}_i^{(2)} \quad (3.11)$$

$$\mathcal{T}'_i = \mathcal{T}_i^{(0)} + g_0 \mathcal{T}_i^{(1)} + g_0^2 \mathcal{T}_i^{(2)} \quad (3.12)$$

Each term of the expansion is given by the sum of various contributions that we enumerate alphabetically with big case latin letters (where needed). Here are the tree-level expressions:

$$\mathcal{T}_i^{(0)} = -i\tilde{q}_i^a \left(\frac{T}{4}, \mathbf{0} \right) T^a \quad (3.13)$$

$$\mathcal{T}'_i^{(0)} = -i\tilde{q}_i^a \left(\frac{3T}{4}, \mathbf{0} \right) T^a \quad (3.14)$$

where repeated indices are summed. The $O(g_0)$ terms are:

$$\mathcal{T}_i^{(1,A)} = \frac{i}{L^3} \sum_{\mathbf{p}} a \sum_{u_0=0}^{T/4-a} \cos\left(\frac{a}{2}p_i\right) \tilde{q}_i^a \left(\frac{T}{4}, \mathbf{p} \right) \tilde{q}_0^b(u_0, -\mathbf{p}) f^{abc} T^c \quad (3.15)$$

$$\mathcal{T}_i^{(1,B)} = \frac{1}{2L^3} \sum_{\mathbf{p}} a^2 \sum_{u_0, v_0=0}^{T/4-a} \dot{p}_i \tilde{q}_0^a(u_0, \mathbf{p}) \tilde{q}_0^b(v_0, -\mathbf{p}) f^{abc} T^c \quad (3.16)$$

$$\mathcal{T}'_i^{(1,A)} = -\frac{i}{L^3} \sum_{\mathbf{p}} a \sum_{u_0=3T/4}^{T-a} \cos\left(\frac{a}{2}p_i\right) \tilde{q}_i^a \left(\frac{3T}{4}, \mathbf{p} \right) \tilde{q}_0^b(u_0, -\mathbf{p}) f^{abc} T^c \quad (3.17)$$

$$\mathcal{T}'_i^{(1,B)} = \frac{1}{2L^3} \sum_{\mathbf{p}} a^2 \sum_{u_0, v_0=3T/4}^{T-a} \dot{p}_i \tilde{q}_0^a(u_0, \mathbf{p}) \tilde{q}_0^b(v_0, -\mathbf{p}) f^{abc} T^c \quad (3.18)$$

And the $O(g_0^2)$ are given by:

$$\mathcal{T}_i^{(2,A)} = -\frac{i}{6} \frac{a^2}{L^6} \sum_{\mathbf{p}, \mathbf{q}} \tilde{q}_i^a \left(\frac{T}{4}, \mathbf{p} \right) \tilde{q}_i^b \left(\frac{T}{4}, \mathbf{q} \right) \tilde{q}_i^c \left(\frac{T}{4}, -\mathbf{p} - \mathbf{q} \right) T^a T^b T^c \quad (3.19)$$

$$\mathcal{T}_i^{(2,B)} = \frac{i}{L^6} \sum_{\mathbf{p}, \mathbf{q}} a^2 \sum_{u_0, v_0=0}^{T/4-a} \cos\left[\frac{a}{2}(p_i - q_i)\right] \tilde{q}_0^a(u_0, \mathbf{p}) \tilde{q}_i^b \left(\frac{T}{4}, -\mathbf{p} - \mathbf{q} \right) \tilde{q}_0^c(v_0, \mathbf{q}) T^a T^b T^c \quad (3.20)$$

$$\begin{aligned} \mathcal{T}_i^{(2,C)} = & -\frac{i}{L^6} \sum_{\mathbf{p}, \mathbf{q}} a^2 \sum_{u_0 \leq v_0=0}^{T/4-a} c(u_0, v_0) \left\{ \cos \left[\frac{a}{2} (p_i + q_i) \right] \tilde{q}_0^a(u_0, \mathbf{p}) \tilde{q}_0^b(v_0, \mathbf{q}) \times \right. \\ & \times \left. \tilde{q}_i^c \left(\frac{T}{4}, -\mathbf{p} - \mathbf{q} \right) + \cos \left(\frac{a}{2} p_i \right) \tilde{q}_i^a \left(\frac{T}{4}, \mathbf{p} \right) \tilde{q}_0^b(v_0, \mathbf{q}) \tilde{q}_0^c(u_0, -\mathbf{p} - \mathbf{q}) \right\} T^a T^b T^c \end{aligned} \quad (3.21)$$

$$\mathcal{T}_i^{\prime(2,A)} = -\frac{i}{6} \frac{a^2}{L^6} \sum_{\mathbf{p}, \mathbf{q}} \tilde{q}_i^a \left(\frac{3T}{4}, \mathbf{p} \right) \tilde{q}_i^b \left(\frac{3T}{4}, \mathbf{q} \right) \tilde{q}_i^c \left(\frac{3T}{4}, -\mathbf{p} - \mathbf{q} \right) T^a T^b T^c \quad (3.22)$$

$$\begin{aligned} \mathcal{T}_i^{\prime(2,B)} = & \frac{i}{L^6} \sum_{\mathbf{p}, \mathbf{q}} a^2 \sum_{u_0, v_0=3T/4}^{T-a} \cos \left[\frac{a}{2} (p_i - q_i) \right] \tilde{q}_0^a(u_0, \mathbf{p}) \tilde{q}_i^b \left(\frac{3T}{4}, -\mathbf{p} - \mathbf{q} \right) \times \\ & \times \tilde{q}_0^c(v_0, \mathbf{q}) T^a T^b T^c \end{aligned} \quad (3.23)$$

$$\begin{aligned} \mathcal{T}_i^{\prime(2,C)} = & -\frac{i}{L^6} \sum_{\mathbf{p}, \mathbf{q}} a^2 \sum_{u_0 \geq v_0=3T/4}^{T-a} c(u_0, v_0) \left\{ \cos \left[\frac{a}{2} (p_i + q_i) \right] \tilde{q}_0^a(u_0, \mathbf{p}) \tilde{q}_0^b(v_0, \mathbf{q}) \times \right. \\ & \times \left. \tilde{q}_i^c \left(\frac{3T}{4}, -\mathbf{p} - \mathbf{q} \right) + \cos \left(\frac{a}{2} p_i \right) \tilde{q}_i^a \left(\frac{3T}{4}, \mathbf{p} \right) \tilde{q}_0^b(v_0, \mathbf{q}) \tilde{q}_0^c(u_0, -\mathbf{p} - \mathbf{q}) \right\} T^a T^b T^c \end{aligned} \quad (3.24)$$

where

$$c(u_0, v_0) = \begin{cases} 1 & \text{if } u_0 \neq v_0 \\ \frac{1}{2} & \text{if } u_0 = v_0 \end{cases} \quad (3.25)$$

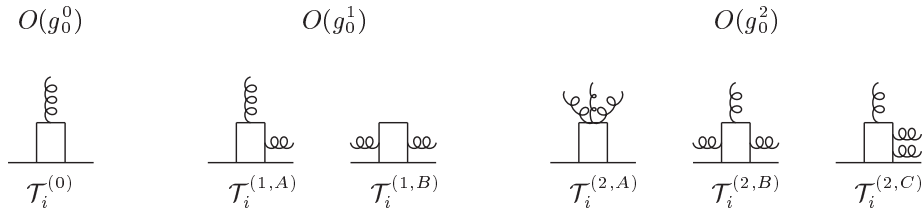


Fig. 3. The contributions to the perturbative expansion of \mathcal{T}_i up to $O(g_0^2)$.

A graphical representation of the Feynman rules for the source at $x_0 = 0$ is reported in Fig. 3 and the source at $x_0 = T$ has an analogous graphical interpretation. From (3.13) and (3.14) one can see that the tree-level of the gluon sources is a gluon field at time $x_0 = T/4$ or $x_0 = 3T/4$ with

spatial polarization and zero momentum. We have now all the ingredients that allow to perform a perturbative one loop calculation of the renormalization constants of the singlet operators and of the correlation functions involving only the sources.

4. Renormalization

The renormalization condition connects the bare operators on the lattice to finite operators renormalized at a scale $\mu = 1/L$:

$$\mathcal{O}_l^R(\mu) = Z_{lk}(\mu a) \mathcal{O}_k(a) \quad (4.1)$$

As we have discussed above, in the flavor singlet sector (and in the *unquenched* case) there is a mixing between the quark (2.13) and the gluon operator (2.14) with the same quantum numbers. We thus write

$$\mathcal{O}_q^R = Z_{qq} \mathcal{O}_q + Z_{qg} \mathcal{O}_g \quad (4.2)$$

$$\mathcal{O}_g^R = Z_{gq} \mathcal{O}_q + Z_{gg} \mathcal{O}_g \quad (4.3)$$

We adopt the following renormalization conditions in the SF scheme:

$$\langle \mathcal{O}_q^R(\mu) \mathbb{S}_q \rangle|_{\mu=1/L} = \langle \mathcal{O}_q(a) \mathbb{S}_q \rangle|^{tree} \quad (4.4)$$

$$\langle \mathcal{O}_q^R(\mu) \mathbb{S}_g \rangle|_{\mu=1/L} = \langle \mathcal{O}_q(a) \mathbb{S}_g \rangle|^{tree} = 0 \quad (4.5)$$

$$\langle \mathcal{O}_g^R(\mu) \mathbb{S}_q \rangle|_{\mu=1/L} = \langle \mathcal{O}_g(a) \mathbb{S}_q \rangle|^{tree} = 0 \quad (4.6)$$

$$\langle \mathcal{O}_g^R(\mu) \mathbb{S}_g \rangle|_{\mu=1/L} = \langle \mathcal{O}_g(a) \mathbb{S}_g \rangle|^{tree} \quad (4.7)$$

From eqs. (4.2) – (4.3) and (4.4) – (4.7), the renormalization constants can be written for $a/L \ll 1$ in the form [14]

$$Z_{qq}(a/L) = 1 - \frac{\alpha_S}{4\pi} C_F \left[\frac{16}{3} \log \frac{a}{L} + B_{qq} + O\left(\frac{a}{L}\right) \right] + O(\alpha_S^2) \quad (4.8)$$

$$Z_{qg}(a/L) = -\frac{\alpha_S}{4\pi} N_f \left[\frac{4}{3} \log \frac{a}{L} + B_{qg} + O\left(\frac{a}{L}\right) \right] + O(\alpha_S^2) \quad (4.9)$$

$$Z_{gg}(a/L) = -\frac{\alpha_S}{4\pi} C_F \left[\frac{16}{3} \log \frac{a}{L} + B_{gg} + O\left(\frac{a}{L}\right) \right] + O(\alpha_S^2) \quad (4.10)$$

$$Z_{gg}(a/L) = 1 - \frac{\alpha_S}{4\pi} \left[N_f \left(\frac{4}{3} \log \frac{a}{L} + B_{gg}^f \right) + N_c B_{gg}^g + O\left(\frac{a}{L}\right) \right] + O(\alpha_S^2) \quad (4.11)$$

where $C_F = 4/3$ and $\alpha_S = g^2/4\pi$. The coefficients of the logarithms represent the *anomalous dimensions* of the corresponding operators. They are responsible for the RG-evolution of the coefficient functions. The B 's are fixed by the renormalization conditions of eqs. (4.4) – (4.7).

4.1 Correlation functions

In order to define the correlation functions for the calculation of the singlet renormalization constants, according to eq. (2.16), we introduce the following four correlation functions

$$f_{qq}(x_0, \mathbf{p}^+) = -a^6 \sum_{\mathbf{y}, \mathbf{z}} e^{i\mathbf{p} \cdot (\mathbf{y} - \mathbf{z})} \left\langle \frac{1}{4} \bar{\psi}(\mathbf{x}) \gamma_{[1} \overleftrightarrow{D}_{2]} \psi(\mathbf{x}) \bar{\zeta}(\mathbf{y}) \gamma_2 \zeta(\mathbf{z}) \right\rangle \quad (4.12)$$

$$f_{qg}(x_0, \mathbf{p}^+) = -a^6 \sum_{\mathbf{y}, \mathbf{z}} e^{i\mathbf{p} \cdot (\mathbf{y} - \mathbf{z})} \left\langle \sum_{\rho} \text{tr} \{ F_{[1\rho}(\mathbf{x}) F_{\rho 2]}(\mathbf{x}) \} \bar{\zeta}(\mathbf{y}) \gamma_2 \zeta(\mathbf{z}) \right\rangle \quad (4.13)$$

$$f_{gg}(x_0) = \left\langle \frac{1}{4} \bar{\psi}(x) \gamma_{[1} \overleftrightarrow{D}_{2]} \psi(x) \text{tr} \{ \mathcal{T}_1 \mathcal{T}_2 \} \right\rangle \quad (4.14)$$

$$f_{gg}(x_0) = \left\langle \sum_{\rho} \text{tr} \{ F_{[1\rho}(x) F_{\rho 2]}(x) \} \text{tr} \{ \mathcal{T}_1 \mathcal{T}_2 \} \right\rangle \quad (4.15)$$

In the correlation functions (4.12) and (4.13) we perform the computation with $\mathbf{p} = 0$ and $\boldsymbol{\theta} = (\theta_1, 0, 0)$. Moreover, we are free to choose the physical distance x_0 of the operator insertions from the lower boundary, and we fix $x_0 = T/2$ in all the correlation functions. We have also to define correlation functions which involve the sources both at $x_0 = 0$ and $x_0 = T$, because the correlation functions (4.12) – (4.15) have to be properly normalized by removing the renormalization of the sources. The quark source has a well known logarithmic divergence [9,13]. Our gluon source, as it will be seen, has a leading linear divergence. The correlation function for the quark source is

$$f_1 = -\frac{a^{12}}{L^6} \sum_{\mathbf{u}, \mathbf{v}, \mathbf{y}, \mathbf{z}} \langle \bar{\zeta}'(\mathbf{u}) \gamma_5 \zeta'(\mathbf{v}) \bar{\zeta}(\mathbf{y}) \gamma_5 \zeta(\mathbf{z}) \rangle \quad (4.16)$$

and for the gluon source:

$$G_1 = \frac{1}{L^8} \langle \mathcal{S} \mathcal{S}' \rangle \quad (4.17)$$

where \mathcal{S} and \mathcal{S}' are defined in (3.1) and (3.4). We can calculate analytically the tree-level of the diagonal correlation functions f_{qq} and f_{gg} and of the sources correlation functions f_1 and G_1 . The tree-level of f_1 with $\mathbf{p} = \boldsymbol{\theta} = 0$ and $m_0 = 0$ is

$$f_1^{(0)} = N_c \quad (4.18)$$

where N_c is the number of colors. The tree-level of G_1 is

$$G_1^{(0)} = \left(\frac{T}{L} \right)^2 \frac{N_c^2 - 1}{1024} \quad (4.19)$$

The tree-level of G_1 is a constant and therefore the same on the lattice and on the continuum. The correlation functions with a non zero tree-level are $f_{qq}(x_0; \theta_1)$ and $f_{gg}(x_0)$. The *tree-level* of f_{qq} is

$$f_{qq}^{(0)}(x_0; \theta_1) = \frac{i \hat{p}_1^+ N_c}{R(p^+)^2} \left[(-i \hat{p}_0) \left(M_-(p^+) e^{-2\omega(\mathbf{p}^+)x_0} - M_+(p^+) e^{-2\omega(\mathbf{p}^+)(2T-x_0)} \right) \right] \Big|_{\mathbf{p}=0} \quad (4.20)$$

and in the continuum and chiral limit it takes the form

$$f_{qq}^{(0)}(x_0; \theta_1) = \frac{\theta_1}{L} \frac{N_c}{(1 + e^{-2\frac{\theta_1}{L}T})^2} \left[e^{-2\frac{\theta_1}{L}x_0} + e^{-2\frac{\theta_1}{L}(2T-x_0)} \right]. \quad (4.21)$$

The purely gluonic correlation function has a tree-level of the form

$$f_{gg}^{(0)}(x_0) = \frac{N_c^2 - 1}{16a^2} [d_{11}(x_0 + a, T/4; \mathbf{0}) - d_{11}(x_0 - a, T/4; \mathbf{0})] \times \\ \times [d_{22}(x_0 + a, T/4; \mathbf{0}) - d_{22}(x_0 - a, T/4; \mathbf{0})] \quad (4.22)$$

where $d_{\mu\mu}(y_0, z_0; \mathbf{q})$ is the time-momentum gluon propagator connecting y_0 and z_0 time slices, carrying a momentum \mathbf{q} and polarization μ [9]. Eq. (4.22) is the square of the time lattice derivative of the spatial gluon propagator. The fact that the spatial gluon propagator with zero momentum is linear in time coordinates [9], implies that with $x_0 \pm a > T/4$, the expression of $f_{gg}^{(0)}(x_0)$ is independent of x_0 and reads

$$f_{gg}^{(0)}(x_0) = \frac{N_c^2 - 1}{64} \quad (4.23)$$

Lattice and continuum expressions are identical.

4.2 One loop perturbative expansion

The only missing ingredients to perform a one loop perturbative expansion of the correlation functions (4.12) – (4.15) and (4.16) – (4.17) are the Feynman rules coming from the expansion of the operators and from the gauge part of the action. In Appendix A we give the perturbative expansion of the field strength $F_{\mu\nu}$ to first order. The second order is rather cumbersome and not so instructive. In Appendix B we give the Feynman rules of the gauge part of the action. The expansion of f_1 was already done in [9], while the expansion of f_{qq} is actually the same performed in the non singlet calculation [13]. In the following, we will restrict the attention to the new correlation functions.

i) G_1

The correlation function involving only gluon sources, G_1 , defined in (4.17), can be expanded in terms of the perturbative expansion of \mathcal{S} , \mathcal{S}' and the action. The Feynman diagrams of the expansion of this correlation function are given in Fig. 4. There are two checks of the calculation. The gluon self-energy develops quadratic divergences that cancel out by summing all the self-energy contributions (cfr. diagrams 6.a – 6.g in Fig. 4), and the cancellation has to take place

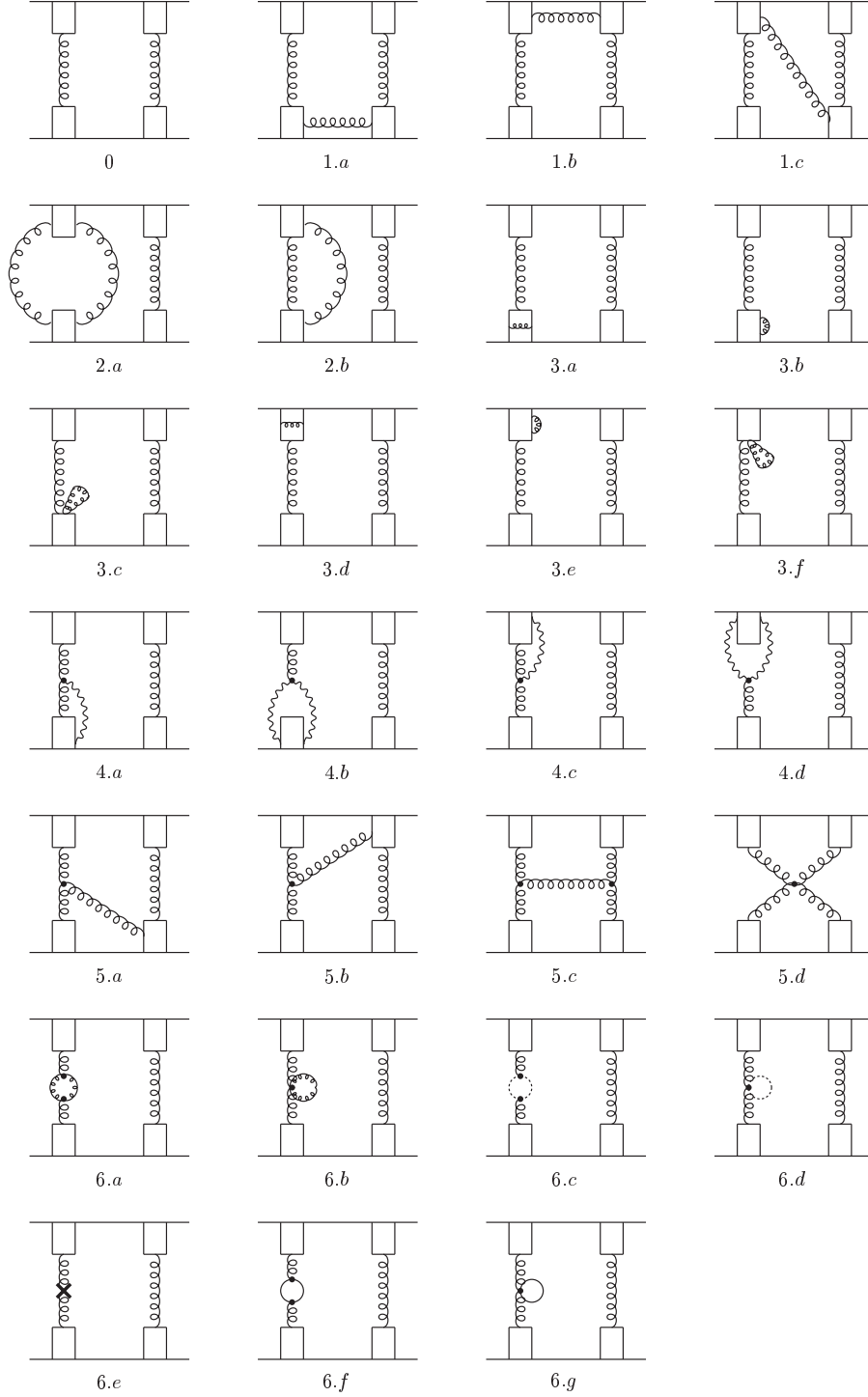


Fig. 4. Feynman diagrams of the one loop expansion of G_1 .

separately in the gluon sector (cfr. diagrams 6.a – 6.e) and in the fermion one (cfr. diagrams 6.f – 6.g). This is verified in our computation.

The second check is specific to our definition of the gluon source. As anticipated in section 2, the source develops linear divergences that must cancel once we normalize f_{gg} with $\sqrt{G_1}$ and they do so. Numerical results for the ratio

$$\frac{G_1^{(1)}}{G_1^{(0)}} = R_1^{(gl)} + N_f R_1^{(fe)} \quad (4.24)$$

are reported in Table 1, where it can be seen the presence of linear divergences in $R_1^{(gl)}$.

ii) f_{qg}

The correlation function f_{qg} , concerning the gluon operator with the quark source, eq. (4.13), can be expressed through [9]

$$\begin{aligned} [\zeta(\mathbf{x})\bar{\zeta}(\mathbf{y})]_F &= P_- U_0(x - a\hat{0}) S(x, y) U_0(y - a\hat{0}) P_+ |_{x_0=y_0=a} + \\ &\quad - \frac{1}{2} P_- \gamma_k (\partial_k + \partial_k^*) a^{-2} \delta_{\mathbf{xy}} \end{aligned} \quad (4.25)$$

which has to be expanded to the $O(g_0^2)$ order. It also requires the tree-level of the gluon operator in the time-momentum scheme, which can be easily computed through the field strength expression given in Appendix A. A picture of the Feynman diagrams for f_{qg} is reported in Fig. 5. For the computation of this correlation function, as in the case of f_{qq} [13], we use a *finite-size* momentum $\boldsymbol{\theta} = (0.1, 0, 0)$.

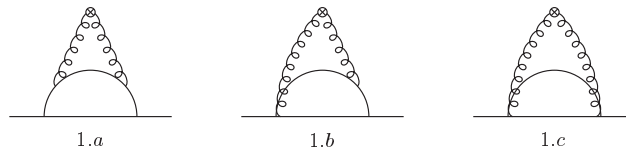


Fig. 5. Feynman diagrams of the one loop expansion of f_{qg} .

The expressions of the Feynman diagrams are quite involved, not so instructive and will not be shown. Numerical results of $f_{qg}^{(1)}/f_{qg}^{(0)}$ are reported in Table 2.

iii) f_{gq}

The second non diagonal correlation function, f_{gq} is defined through eq. (4.14). Its computation involves only the tree-level of the gluon source. It depends on x_0 but not on the momentum,

because the gluon source is projected to zero momentum. The expansion of the quark operator was already done in [13]. Feynman diagrams are depicted in Fig. 6. Numerical results are parametrized as

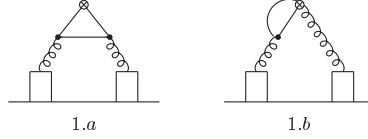


Fig. 6. Feynman diagrams of the one loop expansion of f_{gq} .

$$\frac{f_{gq}^{(1)}}{f_{gg}^{(0)}} = N_f R_{gq}^{(fe)} \quad (4.26)$$

because this correlation function is proportional to the number of dynamical fermions. Note that the value of $f_{gq}^{(1)}/f_{gq}^{(0)}$ is available for lattices with size multiple of two while $R_{gq}^{(fe)}$ is available for lattices with size multiple of four, because correlation functions with the gluon source involve $T/4$ as an integer parameter, while for the quark source they do not. Numerical results are reported in Table 2.

iv) f_{gg} The calculation of this gluonic correlation function, eq. (4.15), is technically difficult. We have to use the expansion of the gluon source, eqs. (3.13) – (3.21), and of the operator up to the second order. We can do here the same checks that we have done for G_1 . Indeed, the quadratic divergences cancel out by summing all the self-energy contributions (cfr. diagrams 5.a – 5.g in Fig. 7), and the cancellation takes place separately in the gluon sector (cfr. diagrams 5.a – 5.e) and in the fermion one (cfr. diagrams 5.f – 5.g). Linear divergences cancel out once we normalize f_{gg} with $\sqrt{G_1}$. Numerical results are presented in Table 3 by parametrizing them as follows

$$\frac{f_{gg}^{(1)}}{f_{gg}^{(0)}} = R_{gg}^{(gl)} + N_f R_{gg}^{(fe)} \quad (4.27)$$

Note that $R_{gg}^{(gl)}$ has a linear divergence while $R_{gg}^{(fe)}$ has only a logarithmic one.

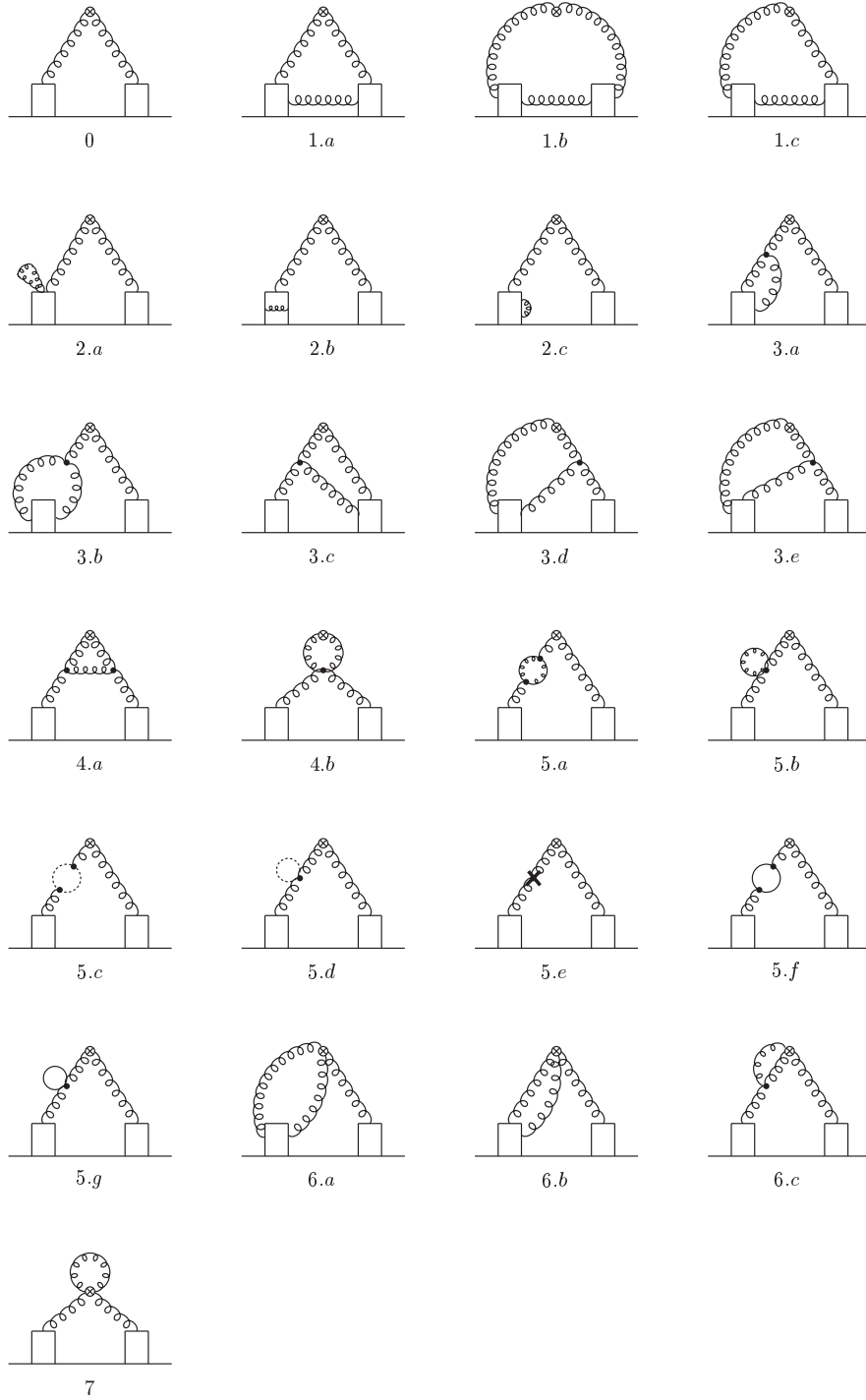


Fig. 7. Feynman diagrams of the one loop expansion of f_{gg} .

4.3 Renormalization constants

In order to renormalize the correlation functions (4.12) – (4.15), we first have to express the bare

parameters m_0 and g_0 through the renormalized ones. In a mass independent renormalization scheme, we have

$$g_R^2 = g_0^2 Z_g(g_0^2, a\mu) \quad (4.28)$$

$$m_R = m_q Z_m(g_0^2, a\mu), \quad m_q = m_0 - m_c \quad (4.29)$$

We choose

$$m_R = 0 \quad (4.30)$$

To the order considered, the required substitution is then given by

$$g_0^2 = g_R^2 + O(g_R^4) \quad (4.31)$$

With $m_R = 0$, we have

$$m_0 = m_c^{(1)} g_R^2 + O(g_R^4) \quad (4.32)$$

For the value of $m_c^{(1)}$, we take the one computed in [15]

$$am_c^{(1)} = -0.4342856(3) \quad (4.33)$$

We are now ready to extract the renormalization constants of the flavor singlet operators. We define the normalized correlation functions:

$$h_{qq} = \frac{f_{qq}}{\sqrt{f_1}}, \quad h_{qg} = \frac{f_{qg}}{\sqrt{f_1}} \quad (4.34)$$

$$h_{gg} = \frac{f_{gg}}{\sqrt{G_1}}, \quad h_{gq} = \frac{f_{gq}}{\sqrt{G_1}} \quad (4.35)$$

The relations between the operators and the renormalization constants (4.2) and (4.3) for the correlation functions are

$$h_{\alpha\beta}^{(R)} = \sum_{\gamma=q,g} Z_{\alpha\gamma} h_{\beta\gamma}, \quad \alpha, \beta = q, g \quad (4.36)$$

The generic expansion of the f , h and Z functions is

$$f = f^{(0)} + g_0^2 f^{(1)} + O(g_0^4) \quad (4.37)$$

$$h = h^{(0)} + g_0^2 h^{(1)} + O(g_0^4) \quad (4.38)$$

$$Z = Z^{(0)} + g_0^2 Z^{(1)} + O(g_0^4) \quad (4.39)$$

For h_{qg} or h_{gq} , $h^{(0)} = 0$. For Z_{qq} or Z_{gg} , $Z^{(0)} = 1$, and for Z_{qg} and Z_{gq} , $Z^{(0)} = 0$. By expanding eqs. (4.36) to order $O(g_R^2)$, we have

$$\begin{aligned} h_{qq}^{(R)}(x_0, \theta) &= h_{qq}^{(0)} + g_R^2 \left\{ h_{qq}^{(1)} + \frac{\partial m_0}{\partial g_R^2} \frac{\partial}{\partial m_0} h_{qq}^{(0)} + Z_{qq}^{(1)} h_{qq}^{(0)} \right\} + O(g_R^4) \\ &= h_{qq}^{(0)} + g_R^2 \left\{ h_{qq}^{(1)} + m_c^{(1)} \frac{\partial}{\partial m_0} h_{qq}^{(0)} + Z_{qq}^{(1)} h_{qq}^{(0)} \right\} + O(g_R^4) \end{aligned} \quad (4.40)$$

$$h_{gq}^{(R)}(x_0) = g_R^2 \left\{ h_{gq}^{(1)} + Z_{gq}^{(1)} h_{gq}^{(0)} \right\} + O(g_R^4) \quad (4.41)$$

$$h_{qg}^{(R)}(x_0, \theta) = g_R^2 \left\{ h_{qg}^{(1)} + Z_{qg}^{(1)} h_{qg}^{(0)} \right\} + O(g_R^4) \quad (4.42)$$

$$h_{gg}^{(R)}(x_0) = h_{gg}^{(0)} + g_R^2 \left\{ h_{gg}^{(1)} + Z_{gg}^{(1)} h_{gg}^{(0)} \right\} + O(g_R^4) \quad (4.43)$$

where the amplitudes (4.40), (4.41) and (4.42) on the right hand side are to be evaluated at $m_0 = 0$. In order to avoid technical problems without compromising the precision, we put $m_0 = 1.0 \times 10^{-10}$ in our programs.

The renormalization conditions for the h 's read

$$h_{qq}^{(R)} = h_{qq}^{(0)}, \quad \text{with } x_0 = L/2, \quad \theta_1 = 0.1, \quad \mu = 1/L \quad (4.44)$$

$$h_{qg}^{(R)} = 0, \quad \text{with } x_0 = L/2, \quad \theta_1 = 0.1, \quad \mu = 1/L \quad (4.45)$$

$$h_{gq}^{(R)} = 0, \quad \text{with } x_0 = L/2, \quad \mu = 1/L \quad (4.46)$$

$$h_{gg}^{(R)} = h_{gg}^{(0)}, \quad \text{with } x_0 = L/2, \quad \mu = 1/L \quad (4.47)$$

Since the only dependence on the lattice spacing is through the combination a/L , the continuum limit is equivalent to the limit $L/a \rightarrow \infty$, i.e. the number of points $N \rightarrow \infty$. By imposing the renormalization conditions (4.44) – (4.47), we obtain

$$Z_{qq}^{(1)}\left(\theta_1, \frac{x_0}{L}, \frac{a}{L}\right) = -\frac{f_{qq}^{(1)}}{f_{qq}^{(0)}} - m_c^{(1)} \frac{1}{f_{qq}^{(0)}} \frac{\partial f_{qq}^{(0)}}{\partial m_0} + \frac{1}{2} \frac{f_1^{(1)}}{f_1^{(0)}} \quad (4.48)$$

$$Z_{qg}^{(1)}\left(\frac{x_0}{L}, \frac{a}{L}\right) = -\frac{f_{gq}^{(1)}}{f_{gq}^{(0)}} \quad (4.49)$$

$$Z_{gg}^{(1)}\left(\theta_1, \frac{x_0}{L}, \frac{a}{L}\right) = -\frac{f_{gg}^{(1)}}{f_{gg}^{(0)}} \quad (4.50)$$

$$Z_{gg}^{(1)}\left(\frac{x_0}{L}, \frac{a}{L}\right) = -\frac{f_{gg}^{(1)}}{f_{gg}^{(0)}} + \frac{1}{2} \frac{G_1^{(1)}}{G_1^{(0)}} \quad (4.51)$$

5. Analysis and results

In order to separate the logarithmic coefficients from the finite terms in the renormalization constants (4.47) – (4.50), and to get rid of the lattice artefacts embedded in their own definition, we apply a technique based on combinations of the Z 's at different values of $N = L/a$ [9, 18]. From general arguments, it is known that the N dependence including lattice artefacts can be parametrized as follows

$$Z^{(1)}(N) = A + B \log(N) + \sum_{k=1}^{\infty} \frac{1}{N^k} \{C_k + D_k \log(N)\}, \quad N = \frac{L}{a} \quad (5.1)$$

where all the coefficients of the expansion depend on the details of the calculation (boundary conditions, operator representations, etc.), except for B , which is related to the leading anomalous dimension and is therefore scheme independent. In order to check that our Z 's reproduce the correct logarithmic coefficients, we introduce a numerical *logarithmic* derivative

$$\Delta^{(0)}(N) \equiv \frac{N}{2\eta} [Z^{(1)}(N+\eta) - Z^{(1)}(N-\eta)] \quad (5.2)$$

with $\eta = 2$ for $Z_{qq}^{(1)}$ or $Z_{gq}^{(1)}$ and $\eta = 4$ for $Z_{gg}^{(1)}$ or $Z_{gg}^{(1)}$, depending upon the presence of fermion or gluon sources, which are computed respectively on lattice sizes multiple of two or four. The quantity $\Delta^{(0)}(N)$ slowly approaches B with a rate proportional to $1/N$. Infact, it can be expanded according to

$$\Delta^{(0)}(N) = B + \tilde{C}_1 g^{(0)}(N) + \tilde{D}_1 h^{(0)}(N) + \tilde{C}_2 e^{(0)}(N) + \tilde{D}_2 m^{(0)}(N) + O\left(\frac{1}{N^3}\right) \quad (5.3)$$

with new coefficients and the auxiliary functions

$$\begin{aligned} g^{(0)}(N) &= \frac{1}{N}, & h^{(0)}(N) &= \frac{1}{N} \log(N) \\ e^{(0)}(N) &= \frac{1}{N^2}, & m^{(0)}(N) &= \frac{1}{N^2} \log(N) \end{aligned} \quad (5.4)$$

In order to have a safe continuum extrapolation of (5.3), terms of order $O(1/N)$ should be absent. This can be arranged with a simple procedure. The first step consists in building the quantity

$$\Delta^{(1)}(N) \equiv \frac{\Delta^{(0)}(N)g^{(0)}(N+\eta) - \Delta^{(0)}(N+\eta)g^{(0)}(N)}{g^{(0)}(N+\eta) - g^{(0)}(N)} \quad (5.5)$$

which, by the same token, can be expanded as

$$\Delta^{(1)}(N) = B + \hat{C}_1 g^{(1)}(N) + \hat{C}_2 h^{(1)}(N) + \hat{D}_2 e^{(1)}(N) + O\left(\frac{1}{N^3}\right) \quad (5.6)$$

where a new set of coefficients and auxiliary functions

$$g^{(1)}(N) = \frac{1}{2} \log\left(1 + \frac{\eta}{N}\right); \quad h^{(1)}(N), e^{(1)}(N) \xrightarrow{N \rightarrow \infty} O\left(\frac{1}{N^2}\right) \quad (5.7)$$

have been introduced. Note that, at this point, the only auxiliary function of order $O(1/N)$ is $g^{(1)}(N)$, and it can be removed with a second subtraction step, analogous to the previous one.

By defining

$$\Delta^{(2)}(N) \equiv \frac{\Delta^{(1)}(N)g^{(1)}(N+\eta) - \Delta^{(1)}(N+\eta)g^{(1)}(N)}{g^{(1)}(N+\eta) - g^{(1)}(N)} \quad (5.8)$$

one can easily convince himself that all the terms of order $O(1/N)$ have been removed, so that

$$\Delta^{(2)}(N) = B + O\left(\frac{1}{N^2}\right) \quad (5.9)$$

and the logarithmic coefficient B can be extracted with a good precision through an ordinary fit. Obviously, every subtraction step cancels out part of the result, and a big precision is required in order to avoid rounding effects. For this reason, all the computations have been done in double precision, as shown in Tables 1 – 3. Numerical results for the anomalous dimensions are reported on second column of Table 4, and are compared with their analytic values, obtained from dimensional regularization. It has to be noted that $\gamma_{gg}^{(gl)} = 0$ and this is verified with a good precision by our computation. The results for γ_{qq} are omitted, because they are the same ones as in the non singlet calculation, and can be found in [13].

The extraction of the correct logarithmic coefficients shows the consistency of the calculation. The determination of the finite scheme dependent terms is obtained by subtracting the logarithmic divergences with the exact coefficients. This generates the *subtracted renormalization constants*

$$Z_{\text{sub}}^{(1)}(N) = A + \sum_{k=1}^{\infty} \frac{1}{N^k} \{C_k + D_k \log(N)\} \quad (5.10)$$

that are again combined in order to suppress lattice artefacts. Following eqs. (4.8) – (4.11), we parametrize our continuum results as

$$Z_{qq}(a/L) = 1 + g_R^2 \left(\gamma_{qq} \log \frac{a}{L} + B_{qq}^{SF} \right) \quad (5.11)$$

$$Z_{qg}(a/L) = g_R^2 N_f \left(\gamma_{qg} \log \frac{a}{L} + B_{qg}^{SF} \right) \quad (5.12)$$

$$Z_{gq}(a/L) = g_R^2 \left(\gamma_{gq} \log \frac{a}{L} + B_{gq}^{SF} \right) \quad (5.13)$$

$$Z_{gg}(a/L) = 1 + g_R^2 \left[N_f \left(\gamma_{gg}^{(fe)} \log \frac{a}{L} + [B_{gg}^{SF}]^{(fe)} \right) + \gamma_{gg}^{(gl)} \log \frac{a}{L} + [B_{gg}^{SF}]^{(gl)} \right] \quad (5.14)$$

The values of the extrapolated $B_{\alpha\beta}^{SF}$ ($\alpha, \beta = q, g$) are reported on first column of Table 4. Again, $B_{qq}^{(SF)}$ is omitted, because it can be found in [13].

The impact of lattice artefacts on the continuum approach of the finite coefficients $B_{\alpha\beta}^{SF}$ can be estimated dividing $Z_{\text{sub}}^{(1)}$ by the continuum fit of the finite coefficients. We introduce the following *test* functions

$$\sigma_{gg}^{(fe)} \left(\frac{L}{a} \right) = \frac{[Z_{gg}^{(1)}]^{(fe)} - \gamma_{gg}^{(fe)} \log \frac{a}{L}}{[B_{gg}^{SF}]^{(fe)}} \quad (5.15)$$

$$\sigma_{gg}^{(gl)} \left(\frac{L}{a} \right) = \frac{[Z_{gg}^{(1)}]^{(gl)}}{[B_{gg}^{SF}]^{(gl)}} \quad (5.16)$$

$$\sigma_{gq} \left(\frac{L}{a} \right) = \frac{Z_{gq}^{(1)} - \gamma_{gq} \log \frac{a}{L}}{B_{gq}^{SF}} \quad (5.17)$$

$$\sigma_{qg} \left(\frac{L}{a} \right) = \frac{Z_{qg}^{(1)} - \gamma_{qg} \log \frac{a}{L}}{B_{qg}^{SF}} \quad (5.18)$$

which converge to one in the continuum limit and differ from one because of the lattice artefacts. Note that $Z^{(1)}$ and $Z_{\text{sub}}^{(1)}$ coincide for the gluon–gluon correlation, because the anomalous dimension is zero. In each of Figs. 13 – 16 one curve refers to the unimproved case, and the other one shows the effect of the improvement procedure described above. After the suitable combinations, the continuum extrapolation is much more safe.

The finite part of the renormalization constants can be used to match experimental results extracted at high energy in a specific continuum scheme like \overline{MS} and lattice results calculated

nonperturbatively at low energy and evolved to high energy within this particular lattice scheme (the SF scheme). The matching coefficients are given by

$$B_{\alpha\beta}^{\text{match}} = B_{\alpha\beta}^{SF} - B_{\alpha\beta}^{\overline{MS}}, \quad \alpha, \beta = q, g \quad (5.19)$$

The values of $B_{\alpha\beta}^{\overline{MS}}$ can be found in [16] and the matching coefficients come out to be

$$\left\{ \begin{array}{ll} [B_{gg}^{\text{match}}]^{(gl)} &= -0.4697(1) \\ [B_{gg}^{\text{match}}]^{(fe)} &= 0.1044(1) \\ B_{gq}^{\text{match}} &= -0.04162(1) \\ B_{qg}^{\text{match}} &= -0.1195(1) . \end{array} \right. \quad (5.20)$$

This is the result of the calculation.

6. Conclusions

This computation put the premises for a lattice non perturbative calculation of the amount of gluon in a hadron from first principles in the SF scheme. The new definition of a gauge invariant gluon source might also be used for a novel definition of α_s , or for further studies of non perturbative aspects of the gluon propagation. Preliminary numerical simulations show the feasibility of our definition [to appear...].

Acknowledgments

We are grateful to S. Sint and G. de Divitiis for discussions on possible definitions of gluon source operators in the SF scheme. We also express thanks to A. Bucarelli and V. D'Achille for their collaboration in a preliminary stage of the calculation.

Appendix A *Strength tensor perturbative expansion*

In this appendix we report the perturbative expansion of the lattice strength tensor $F_{\mu\nu}$ in time-momentum representation, up to order g_0 . Fourier transforms are required only along the space directions by the absence of periodic boundary conditions in time, which characterizes the SF scheme. This produces an asymmetry between temporal and spatial Lorentz indices and makes the algebra a bit more elaborate. The perturbative expansion is defined by the formula

$$F_{\mu\nu}(x) = \sum_{k=0}^{\infty} g_0^k F_{\mu\nu}^{(k)}(x); \quad F_{\mu\nu}^{(k)}(x) = -F_{\nu\mu}^{(k)}(x), \quad \forall k \in \mathbb{N} \quad (\text{A.1})$$

The $O(g_0^0)$ terms are given by

$$F_{jk}^{(0)}(x) = \frac{i}{a} \frac{1}{L^3} \sum_{\mathbf{p}} e^{i\mathbf{p} \cdot \mathbf{x}} \left[\cos\left(\frac{ap_k}{2}\right) \sin(ap_j) \tilde{q}_k^a(x_0; \mathbf{p}) - \cos\left(\frac{ap_j}{2}\right) \sin(ap_k) \tilde{q}_j^a(x_0; \mathbf{p}) \right] T^a \quad (\text{A.2})$$

$$\begin{aligned} F_{0k}^{(0)}(x) = & \frac{1}{2a} \frac{1}{L^3} \sum_{\mathbf{p}} e^{i\mathbf{p} \cdot \mathbf{x}} \left\{ \cos\left(\frac{ap_k}{2}\right) [\tilde{q}_k^a(x_0 + a; \mathbf{p}) - \tilde{q}_k^a(x_0 - a; \mathbf{p})] + \right. \\ & \left. - i \sin(ap_k) [\tilde{q}_0^a(x_0; \mathbf{p}) + \tilde{q}_0^a(x_0 - a; \mathbf{p})] \right\} T^a \end{aligned} \quad (\text{A.3})$$

and the $O(g_0)$ ones are

$$\begin{aligned} F_{jk}^{(1)}(x) = & \frac{g_0}{4} \frac{1}{L^6} \sum_{\mathbf{p}, \mathbf{q}} e^{i(\mathbf{p} + \mathbf{q}) \cdot \mathbf{x}} \left\{ 2 \left[\cos\left(\frac{ap_j}{2} + aq_j\right) \cos\left(\frac{aq_k}{2}\right) + \cos\left(\frac{aq_k}{2} + ap_k\right) \cos\left(\frac{ap_j}{2}\right) + \right. \right. \\ & \left. \left. - \cos\left(\frac{ap_j}{2}\right) \cos\left(\frac{aq_k}{2}\right) + \cos\left(\frac{ap_j}{2} + aq_j\right) \cos\left(\frac{aq_k}{2} + ap_k\right) \right] \tilde{q}_j^a(x_0; \mathbf{p}) \tilde{q}_k^b(x_0; \mathbf{q}) + \right. \\ & + \sin\left(\frac{ap_j}{2} + \frac{aq_j}{2}\right) [\sin(aq_k) - \sin(ap_k)] \tilde{q}_j^a(x_0; \mathbf{p}) \tilde{q}_j^b(x_0; \mathbf{q}) + \\ & \left. + \sin\left(\frac{ap_k}{2} + \frac{aq_k}{2}\right) [\sin(ap_j) - \sin(aq_j)] \tilde{q}_k^a(x_0; \mathbf{p}) \tilde{q}_k^b(x_0; \mathbf{q}) \right\} \end{aligned} \quad (\text{A.4})$$

$$\begin{aligned}
F_{0k}^{(1)}(x) = & \frac{g_0}{4} \frac{1}{L^6} \sum_{\mathbf{p}, \mathbf{q}} e^{i(\mathbf{p}+\mathbf{q}) \cdot \mathbf{x}} \left\{ \left[\cos\left(\frac{aq_k}{2} + ap_k\right) + \cos\left(\frac{aq_k}{2}\right) \right] \times \right. \\
& \times \left[\tilde{q}_0^a(x_0; \mathbf{p}) \tilde{q}_k^b(x_0 + a; \mathbf{q}) + \tilde{q}_0^a(x_0 - a; \mathbf{p}) \tilde{q}_k^b(x_0 - a; \mathbf{q}) \right] + \\
& + \left[\cos(ap_k + \frac{aq_k}{2}) - \cos\left(\frac{aq_k}{2}\right) \right] \times \\
& \times \left[\tilde{q}_0^a(x_0; \mathbf{p}) \tilde{q}_k^b(x_0; \mathbf{q}) + \tilde{q}_0^a(x_0 - a; \mathbf{p}) \tilde{q}_k^b(x_0; \mathbf{q}) \right] + \\
& + i \sin(ap_k) [\tilde{q}_0^a(x_0; \mathbf{p}) \tilde{q}_0^b(x_0; \mathbf{q}) - \tilde{q}_0^a(x_0 - a; \mathbf{p}) \tilde{q}_0^b(x_0 - a; \mathbf{q})] + \\
& \left. + i \sin\left(\frac{ap_k}{2} + \frac{aq_k}{2}\right) [\tilde{q}_k^a(x_0; \mathbf{p}) \tilde{q}_k^b(x_0 + a; \mathbf{q}) - \tilde{q}_k^a(x_0; \mathbf{p}) \tilde{q}_k^b(x_0 - a; \mathbf{q})] \right\} f^{abc} T^c
\end{aligned} \tag{A.5}$$

Appendix B *Feynman rules for the action*

In this appendix we report the Feynman rules in the time-momentum representation for the gauge part of the action, which never appeared in the literature. The Feynman rules for the fermion one are given in [9]. The gauge part of the action is composed by a pure gauge term, a ghost term and a measure term. The perturbative expansion in powers of g_0 reads

$$S_G[q] = \sum_{k=0}^{\infty} g_0^k S_G^{(k)}[q] \tag{B.1}$$

$$S_m[q] = \sum_{k=1}^{\infty} g_0^{2k} S_m^{(2k)}[q] \tag{B.2}$$

$$S_{FP}[q, c, \bar{c}] = \sum_{k=0}^{\infty} g_0^k S_{FP}^{(k)}[q, c, \bar{c}] \tag{B.3}$$

where every term in the sums of eqs. (B.1) – (B.3) has several contributions in the time-momentum representation, due to the fact that we must separate spatial and temporal Lorentz indices. The gauge action S_G and the ghost action S_{FP} are defined in [9]. The measure term is defined in any standard lattice gauge theory book (see for example [17]).

B.1 Vertices with a non zero continuum limit

The time-momentum representation of the *three-gluons* vertex separates in three contributions

$$S_G^{(1)}[q] = \sum_{i=a,b,c} S_G^{(1,i)}[q] \quad (\text{B.4})$$

with the explicit expressions (Feynman graphs are reported in Fig. 8)

$$S_G^{(1,a)}[q] = \frac{1}{L^6} \sum_{\mathbf{l}, \mathbf{m}} a \sum_{x_0=a}^{T-a} \frac{i}{a} \cos \left[\frac{a}{2} (q_k - p_k) \right] \times \\ \times \cos \left[\frac{a}{2} (p_j + q_j) \right] \tilde{q}_k^a(x_0; -\mathbf{l} - \mathbf{m}) q_j^b(x_0; \mathbf{l}) q_j^c(x_0; \mathbf{m}) f^{abc} \quad (\text{B.5})$$

$$S_G^{(1,b)}[q] = \frac{1}{L^6} \sum_{\mathbf{l}, \mathbf{m}} a \sum_{x_0=a}^{T-a} \frac{1}{a} \cos \left[\frac{a}{2} (p_j + q_j) \right] \times \\ \times \tilde{q}_0^a(x_0; -\mathbf{l} - \mathbf{m}) q_j^b(x_0; \mathbf{l}) q_j^c(x_0 + a; \mathbf{m}) f^{abc} \quad (\text{B.6})$$

$$S_G^{(1,c)}[q] = \frac{1}{L^6} \sum_{\mathbf{l}, \mathbf{m}} a \sum_{x_0=a}^{T-a} \cos \left[\frac{a}{2} (q_k - p_k) \right] \times \\ \times \frac{i}{2a} \left[\tilde{q}_k^a(x_0 + a; -\mathbf{l} - \mathbf{m}) + \tilde{q}_k^a(x_0; -\mathbf{l} - \mathbf{m}) \right] q_0^b(x_0; \mathbf{l}) q_0^c(x_0; \mathbf{m}) f^{abc} \quad (\text{B.7})$$

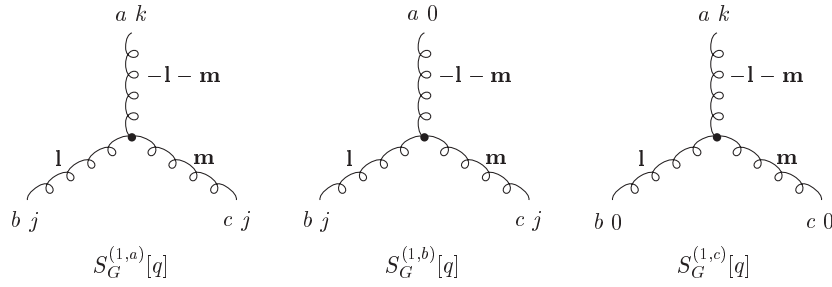


Fig. 8. Feynman diagrams of the three contributions to the *three-gluons* vertex.

The time-momentum representation of the *four-gluon* has many contributions and we report only the ones interested in computing our correlation functions.

$$S_G^{(2)}[q] = \sum_{i=a,b,c} S_G^{(2,i)}[q] \quad (\text{B.8})$$

with the explicit expressions (Feynman graphs are reported in Fig. 9)

$$\begin{aligned} S_G^{(2,a)}[q] = & a^3 \sum_{\mathbf{x}} a \sum_{x_0=a}^{T-a} \frac{1}{L^{12}} \sum_{\mathbf{l}, \mathbf{m}, \mathbf{n}, \mathbf{p}} e^{i(\mathbf{l}+\mathbf{m}+\mathbf{n}+\mathbf{p}) \cdot \mathbf{x}} \times \\ & \times \left\{ 2\tilde{q}_i^a(x_0; \mathbf{l}) \tilde{q}_i^b(x_0; \mathbf{m}) \tilde{q}_j^c(x_0; \mathbf{n}) \tilde{q}_j^d(x_0; \mathbf{p}) \times \right. \\ & \times \left[\cos\left[\frac{a}{2}(l_j + m_j)\right] \cos\left[\frac{a}{2}(n_i + p_i)\right] - \cos\left[\frac{a}{2}(l_i + m_i)\right] \cos\left[\frac{a}{2}(l_j - m_j)\right] + \right. \\ & - \cos\left[\frac{a}{2}(l_j + m_j)\right] \cos\left[\frac{a}{2}(p_i - n_i)\right] - 2\tilde{q}_i^a(x_0; \mathbf{l}) \tilde{q}_j^b(x_0; \mathbf{m}) \tilde{q}_i^c(x_0; \mathbf{n}) \tilde{q}_j^d(x_0; \mathbf{p}) \times \\ & \left. \left. \times \cos\left[\frac{a}{2}(n_i - p_i)\right] \cos\left[\frac{a}{2}(m_j - l_j)\right] \right\} \text{tr}(T^a T^b T^c T^d) \end{aligned} \quad (\text{B.9})$$

$$\begin{aligned} S_G^{(2,b)}[q] = & a^3 \sum_{\mathbf{x}} a \sum_{x_0=a}^{T-a} \frac{1}{L^{12}} \sum_{\mathbf{l}, \mathbf{m}, \mathbf{n}, \mathbf{p}} e^{i(\mathbf{l}+\mathbf{m}+\mathbf{n}+\mathbf{p}) \cdot \mathbf{x}} \times \\ & \times \left\{ 2\tilde{q}_i^a(x_0; \mathbf{l}) \tilde{q}_i^b(x_0; \mathbf{m}) \tilde{q}_0^c(x_0; \mathbf{n}) \tilde{q}_0^d(x_0; \mathbf{p}) \sin\left(\frac{an_i}{2}\right) \sin\left(\frac{ap_i}{2}\right) + \right. \\ & + \tilde{q}_i^a(x_0 + a; \mathbf{l}) \tilde{q}_i^b(x_0; \mathbf{m}) \tilde{q}_0^c(x_0; \mathbf{n}) \tilde{q}_0^d(x_0; \mathbf{p}) \cos\left[\frac{a}{2}(n_i + p_i)\right] + \\ & + \tilde{q}_i^a(x_0; \mathbf{l}) \tilde{q}_i^b(x_0 + a; \mathbf{m}) \tilde{q}_0^c(x_0; \mathbf{n}) \tilde{q}_0^d(x_0; \mathbf{p}) \cos\left[\frac{a}{2}(n_i + p_i)\right] + \\ & - \tilde{q}_i^a(x_0 + a; \mathbf{l}) \tilde{q}_i^b(x_0 + a; \mathbf{m}) \tilde{q}_0^c(x_0; \mathbf{n}) \tilde{q}_0^d(x_0; \mathbf{p}) \cos\left[\frac{a}{2}(n_i + p_i)\right] + \\ & + \tilde{q}_0^a(x_0; \mathbf{n}) \tilde{q}_i^b(x_0 + a; \mathbf{l}) \tilde{q}_i^c(x_0 + a; \mathbf{m}) \tilde{q}_0^d(x_0; \mathbf{p}) \cos\left[\frac{a}{2}(n_i + p_i)\right] + \\ & \left. - 2\tilde{q}_i^a(x_0; \mathbf{l}) \tilde{q}_0^b(x_0; \mathbf{n}) \tilde{q}_i^c(x_0 + a; \mathbf{m}) \tilde{q}_0^d(x_0; \mathbf{p}) \cos\left[\frac{a}{2}(n_i + p_i)\right] \right\} \times \\ & \times \text{tr}(T^a T^b T^c T^d) \end{aligned} \quad (\text{B.10})$$

$$\begin{aligned}
S_G^{(2,c)}[q] = & \frac{a^3}{24} \sum_{\mathbf{x}} a \sum_{x_0=a}^{T-a} \frac{1}{L^{12}} \sum_{\mathbf{l}, \mathbf{m}, \mathbf{n}, \mathbf{p}} e^{i(\mathbf{l}+\mathbf{m}+\mathbf{n}+\mathbf{p}) \cdot \mathbf{x}} \times \\
& \times \left\{ \tilde{q}_i^a(x_0; \mathbf{l}) \tilde{q}_i^b(x_0; \mathbf{m}) \tilde{q}_i^c(x_0; \mathbf{n}) \tilde{q}_i^d(x_0; \mathbf{p}) \times \right. \\
& \times \left[-10 + \sum_{k \neq i} \left(\cos(ap_k) + \cos(al_k) \right) - 12 \sum_{k \neq i} \cos[a(l_k + m_k)] \right] + \\
& - 2\tilde{q}_i^a(x_0 + a; \mathbf{l}) \tilde{q}_i^b(x_0 + a; \mathbf{m}) \tilde{q}_i^c(x_0 + a; \mathbf{n}) \tilde{q}_i^d(x_0 + a; \mathbf{p}) + \\
& + 8\tilde{q}_i^a(x_0; \mathbf{l}) \tilde{q}_i^b(x_0; \mathbf{m}) \tilde{q}_i^c(x_0; \mathbf{n}) \tilde{q}_i^d(x_0 + a; \mathbf{p}) + \\
& + 8\tilde{q}_i^a(x_0; \mathbf{l}) \tilde{q}_i^b(x_0 + a; \mathbf{m}) \tilde{q}_i^c(x_0 + a; \mathbf{n}) \tilde{q}_i^d(x_0 + a; \mathbf{p}) + \\
& \left. - 12\tilde{q}_i^a(x_0; \mathbf{l}) \tilde{q}_i^b(x_0; \mathbf{m}) \tilde{q}_i^c(x_0 + a; \mathbf{n}) \tilde{q}_i^d(x_0 + a; \mathbf{p}) \right\} \times \\
& \times \text{tr}(T^a T^b T^c T^d)
\end{aligned} \tag{B.11}$$

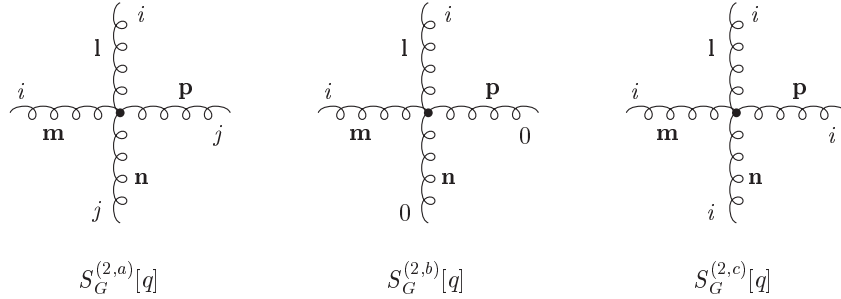


Fig. 9. Feynman diagrams of the three contributions to the *four-gluon* vertex.

Also the ghost term separates in two contributions (which are depicted in Fig. 10):

$$S_{FP}^{(2)}[q, c, \bar{c}] = \sum_{i=a,b} S_{FP}^{(2,i)}[q, c, \bar{c}] \tag{B.12}$$

and these are given by

$$\begin{aligned}
S_{FP}^{(1,a)}[q, c, \bar{c}] = & a \sum_{x_0=a}^{T-a} \frac{1}{L^6} \sum_{\mathbf{l}, \mathbf{m}} i \widehat{(l_k + m_k)} \cos\left(\frac{a}{2} m_k\right) \tilde{c}^a(x_0; -\mathbf{l} - \mathbf{m}) \tilde{q}_k^b(x_0; \mathbf{l}) \times \\
& \times \tilde{c}^c(x_0; \mathbf{m}) f^{abc}
\end{aligned} \tag{B.13}$$

$$\begin{aligned}
S_{FP}^{(1,b)}[q, c, \bar{c}] = & a \sum_{x_0=a}^{T-a} \frac{1}{L^6} \sum_{\mathbf{l}, \mathbf{m}} \tilde{c}^a(x_0; -\mathbf{l} - \mathbf{m}) \frac{1}{2a} \left[\tilde{q}_0^b(x_0; \mathbf{l}) \tilde{c}^c(x_0; \mathbf{m}) + \right. \\
& + \tilde{q}_0^b(x_0; \mathbf{l}) \tilde{c}^c(x_0 + a; \mathbf{m}) - \tilde{q}_0^b(x_0 - a; \mathbf{l}) \tilde{c}^c(x_0 - a; \mathbf{m}) + \\
& \left. - \tilde{q}_0^b(x_0 - a; \mathbf{l}) \tilde{c}^c(x_0; \mathbf{m}) \right] f^{abc}
\end{aligned} \tag{B.14}$$

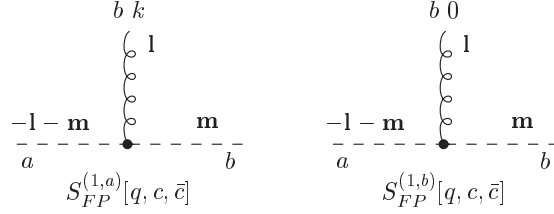


Fig. 10. Feynman diagrams of the two contributions to the *two-ghost – one-gluon* vertex.

B.2 Vertices not existing in the continuum

The measure vertex is given by

$$S_m^{(2)}[q] = \frac{N_c}{12a^2} a \sum_{x_0=a}^{T-a} \frac{1}{L^3} \sum_1 \left[\sum_{k=1,2,3} \left(\tilde{q}_k^a(x_0; \mathbf{l}) q_k^a(x_0; -\mathbf{l}) \right) + q_0^a(x_0; \mathbf{l}) q_0^a(x_0; -\mathbf{l}) \right] \tag{B.15}$$

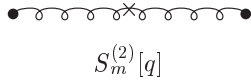


Fig. 11. Feynman diagram of the measure vertex.

The ghost action contributes also with a vertex which has a zero continuum limit. It is made by two contributions (see Fig. 12):

$$S_{FP}^{(2)}[q, c, \bar{c}] = \sum_{i=a,b} S_{FP}^{(2,i)}[q, c, \bar{c}] \tag{B.16}$$

where

$$\begin{aligned}
S_{FP}^{(2,a)}[q, c, \bar{c}] = & \frac{a^2}{12} a \sum_{x_0=a}^{T-a} \frac{1}{L^9} \sum_{\mathbf{l}, \mathbf{m}, \mathbf{n}} \tilde{c}^a(x_0; -\mathbf{l} - \mathbf{m} - \mathbf{n}) (\widehat{l_k + m_k + n_k}) \hat{n}_k \times \\
& \times \tilde{q}_k^b(x_0; \mathbf{l}) \tilde{q}_k^c(x_0; \mathbf{m}) \tilde{c}^d(x_0; \mathbf{n}) f^{abe} f^{cde}
\end{aligned} \tag{B.17}$$

$$\begin{aligned}
S_{FP}^{(2,b)}[q, c, \bar{c}] = & -\frac{1}{12}a \sum_{x_0=a}^{T-a} \frac{1}{L^9} \sum_{\mathbf{l}, \mathbf{m}, \mathbf{n}} \tilde{c}^a(x_0; -\mathbf{l} - \mathbf{m} - \mathbf{n}) \left[q_0^b(x_0; \mathbf{l}) \tilde{q}_0^c(x_0; \mathbf{m}) \tilde{c}^d(x_0 + a; \mathbf{n}) + \right. \\
& - q_0^b(x_0; \mathbf{l}) \tilde{q}_0^c(x_0; \mathbf{m}) \tilde{c}^d(x_0; \mathbf{n}) - q_0^b(x_0 - a; \mathbf{l}) \tilde{q}_0^c(x_0 - a; \mathbf{m}) \tilde{c}^d(x_0; \mathbf{n}) + \\
& \left. + q_0^b(x_0 - a; \mathbf{l}) \tilde{q}_0^c(x_0 - a; \mathbf{m}) \tilde{c}^d(x_0 - a; \mathbf{n}) \right] f^{abe} f^{cde}
\end{aligned} \tag{B.18}$$

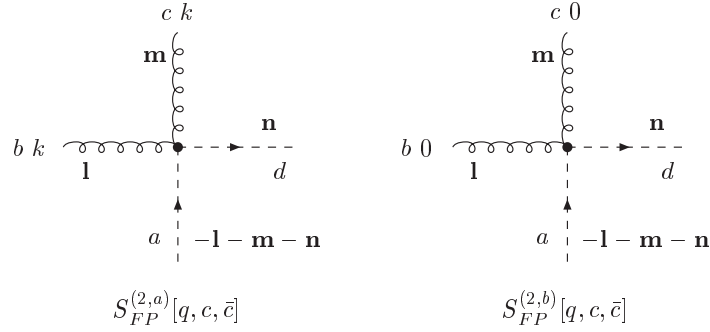


Fig. 12. Feynman diagrams of two contributions to the *two-ghost – two-gluon* vertex.

References

- [1] M. Göckeler et al., Phys. Rev. **D53** (1996) 2317-2325
- [2] C. Best et al., Phys. Rev. **D56** (1997) 2743-2754
- [3] D. Dolgov et al., Nucl. Phys. B (Proc. Suppl.) **94** (2001) 303-306
- [4] D. Dolgov et al., "Moments of Nucleon Light Cone Quark Distributions Calculated in Full Lattice QCD" hep-lat/0201021
- [5] M. Guagnelli et al., Nucl. Phys. **B542** (1999) 395-409
M. Guagnelli et al., Nucl. Phys. **B457** (1999) 153-156
M. Guagnelli et al., Nucl. Phys. **B459** (1999) 594-598
M. Guagnelli et al., Phys. Lett. **B493** (2000) 77-81
- [6] J. Huston et al., Phys. Rev. **D58** (1998) 114034
- [7] R. Petronzio, Nucl. Phys. B (Proc. Suppl.) **83** (2000) 136-139
- [8] M. Lüscher, R. Narayanan, P. Weisz and U. Wolff, Nucl. Phys. **B384** (1992) 168

- S.Sint, Nucl. Phys. **B421** (1994) 135
- [9] M. Lüscher and P. Weisz, Nucl. Phys. **B479** (1996) 429
- [10] M. Baake, B. Gemünden and R.Oedingen, J. Math. Phys. **23** (1982) 944
J.E.Mandula, G.Zweig and J.Govaerts, Nucl. Phys. **B228** (1983) 91
- [11] G. Beccarini, M. Bianchi, S. Capitani and G. Rossi, Nucl. Phys. **B456** (1995) 271
M.Göckeler *et al.*, Phys. Rev. **D54** (1996) 5705
- [12] A. Shindler, Nucl. Phys. B (Proc. Suppl.) **83** (2000) 253-255
- [13] A. Bucarelli, F. Palombi, R. Petronzio and A. Shindler, Nucl. Phys. **B552** (1999) 379
- [14] D.J.Gross e F.Wilczek, Phys. Rep. **D8** (1973) 3633
D.J.Gross and F.Wilczek, Phys. Rep. **D9** (1974) 980
- [15] S. Sint, private notes (1996)
- [16] S. Capitani, G. Rossi Nucl. Phys. B (Proc. Suppl.) **53** (1997) 801-803
- [17] I. Montvay, G. Münster, *Quantum fields on a lattice* (Cambridge University Press)
- [18] M. Lüscher, P. Weisz, Nucl. Phys. **B266** (1986) 309

Table 1. Ratio $G_1^{(1)}/G_1^{(0)}$

| T/a | $R_1^{(gl)}$ | $R_1^{(fe)}$ |
|-------|------------------------------|--------------------------------|
| 4 | $-2.35241571640 \times 10^0$ | $5.43688719630 \times 10^{-1}$ |
| 8 | $-2.89616691565 \times 10^0$ | $2.91628523582 \times 10^{-1}$ |
| 12 | $-3.78563617887 \times 10^0$ | $2.40540867861 \times 10^{-1}$ |
| 16 | $-4.77638846812 \times 10^0$ | $2.18562655437 \times 10^{-1}$ |
| 20 | $-5.81427883554 \times 10^0$ | $2.05144176593 \times 10^{-1}$ |
| 24 | $-6.87867683434 \times 10^0$ | $1.95721360604 \times 10^{-1}$ |
| 28 | $-7.95977357383 \times 10^0$ | $1.88582311080 \times 10^{-1}$ |
| 32 | $-9.05223296007 \times 10^0$ | $1.82902372508 \times 10^{-1}$ |
| 36 | $-1.01528674964 \times 10^1$ | $1.78225084856 \times 10^{-1}$ |
| 40 | $-1.12596369563 \times 10^1$ | $1.74273581484 \times 10^{-1}$ |
| 44 | $-1.23711642225 \times 10^1$ | $1.70868479333 \times 10^{-1}$ |
| 48 | $-1.34864798286 \times 10^1$ | $1.67887576085 \times 10^{-1}$ |
| 52 | $-1.46048775931 \times 10^1$ | $1.65244260811 \times 10^{-1}$ |
| 56 | $-1.57258283938 \times 10^1$ | $1.62875144474 \times 10^{-1}$ |
| 60 | $-1.68489262682 \times 10^1$ | $1.60732582532 \times 10^{-1}$ |

Table 2. Ratios $f_{qg}^{(1)}/f_{qg}^{(0)}$ and $f_{gq}^{(1)}/f_{gq}^{(0)}$

| T/a | $f_{qg}^{(1)}/f_{qg}^{(0)}$ | $R_{gq}^{(fe)}$ |
|-------|---------------------------------|--------------------------------|
| 4 | $-3.90445955289 \times 10^{-2}$ | $1.76632912708 \times 10^{-1}$ |
| 6 | $-5.61960383511 \times 10^{-2}$ | — |
| 8 | $-6.84291322541 \times 10^{-2}$ | $1.29586992658 \times 10^{-1}$ |
| 10 | $-7.81443039581 \times 10^{-2}$ | — |
| 12 | $-8.61855815840 \times 10^{-2}$ | $1.15745211197 \times 10^{-1}$ |
| 14 | $-9.30301253579 \times 10^{-2}$ | — |
| 16 | $-9.89813896977 \times 10^{-2}$ | $1.08336211173 \times 10^{-1}$ |
| 18 | $-1.04242788232 \times 10^{-1}$ | — |
| 20 | $-1.08956354293 \times 10^{-1}$ | $1.03478207253 \times 10^{-1}$ |
| 22 | $-1.13224779604 \times 10^{-1}$ | — |
| 24 | $-1.17124551957 \times 10^{-1}$ | $9.99540929596 \times 10^{-2}$ |
| 26 | $-1.20714100952 \times 10^{-1}$ | — |
| 28 | $-1.24039035245 \times 10^{-1}$ | $9.72321408957 \times 10^{-2}$ |
| 30 | $-1.27135621901 \times 10^{-1}$ | — |
| 32 | $-1.30033166208 \times 10^{-1}$ | $9.50373471243 \times 10^{-2}$ |
| 34 | $-1.32755681834 \times 10^{-1}$ | — |
| 36 | $-1.35323089945 \times 10^{-1}$ | $9.32112990034 \times 10^{-2}$ |
| 38 | $-1.37752097648 \times 10^{-1}$ | — |
| 40 | $-1.40056853184 \times 10^{-1}$ | $9.16554753604 \times 10^{-2}$ |
| 42 | $-1.42249442526 \times 10^{-1}$ | — |
| 44 | $-1.44340271231 \times 10^{-1}$ | $9.03049553605 \times 10^{-2}$ |
| 46 | $-1.46338361917 \times 10^{-1}$ | — |
| 48 | $-1.48251588765 \times 10^{-1}$ | $8.91149749248 \times 10^{-2}$ |
| 50 | $-1.50086864377 \times 10^{-1}$ | — |
| 52 | $-1.51850290135 \times 10^{-1}$ | $8.80535191120 \times 10^{-2}$ |
| 54 | $-1.53547278304 \times 10^{-1}$ | — |
| 56 | $-1.55182651997 \times 10^{-1}$ | $8.70969908092 \times 10^{-2}$ |
| 58 | $-1.56760727661 \times 10^{-1}$ | — |
| 60 | $-1.58285383623 \times 10^{-1}$ | $8.62275524536 \times 10^{-2}$ |

Table 3. Ratio $f_{gg}^{(1)}/f_{gg}^{(0)}$

| T/a | $R_{gg}^{(gl)}$ | $R_{gg}^{(fe)}$ |
|-------|---------------------------------|---------------------------------|
| 4 | $-7.42272842206 \times 10^{-1}$ | $4.32567853743 \times 10^{-2}$ |
| 8 | $-1.03655972167 \times 10^0$ | $-1.42248562169 \times 10^{-2}$ |
| 12 | $-1.47142280292 \times 10^0$ | $-3.03291610705 \times 10^{-2}$ |
| 16 | $-1.95917324599 \times 10^0$ | $-3.89219901277 \times 10^{-2}$ |
| 20 | $-2.47274884132 \times 10^0$ | $-4.48470953718 \times 10^{-2}$ |
| 24 | $-3.00105188219 \times 10^0$ | $-4.93690136333 \times 10^{-2}$ |
| 28 | $-3.53866677061 \times 10^0$ | $-5.30184104212 \times 10^{-2}$ |
| 32 | $-4.08261542990 \times 10^0$ | $-5.60724863587 \times 10^{-2}$ |
| 36 | $-4.63111119327 \times 10^0$ | $-5.86948398012 \times 10^{-2}$ |
| 40 | $-5.18300914136 \times 10^0$ | $-6.09901327477 \times 10^{-2}$ |
| 44 | $-5.73753689001 \times 10^0$ | $-6.30293363500 \times 10^{-2}$ |
| 48 | $-6.29415150120 \times 10^0$ | $-6.48627573963 \times 10^{-2}$ |
| 52 | $-6.85245828489 \times 10^0$ | $-6.65273259871 \times 10^{-2}$ |
| 56 | $-7.41216219458 \times 10^0$ | $-6.80509342931 \times 10^{-2}$ |
| 60 | $-7.97303741242 \times 10^0$ | $-6.94551510343 \times 10^{-2}$ |

Table 4. Constant and logarithmic coefficients as obtained numerically

| | |
|-------------------------------------|---|
| $[B_{gg}^{SF}]^{(gl)} = -0.4613(1)$ | $ \gamma_{gg}^{(gl)} < 5.0 \times 10^{-5}$ |
| $[B_{gg}^{SF}]^{(fe)} = 0.1114(1)$ | $\gamma_{gg}^{(fe)} = -0.0083(1)N_f$ ($-\frac{1}{12\pi^2}N_f = -0.0084434...N_f$) |
| $B_{qg}^{SF} = -0.1167(1)$ | $\gamma_{qg} = -0.0084(1)N_f$ ($-\frac{1}{12\pi^2}N_f = -0.0084434...N_f$) |
| $B_{gq}^{SF} = -0.02614(1)$ | $\gamma_{gq} = -0.04502(1)$ ($-\frac{4}{9\pi^2} = -.045031... $) |

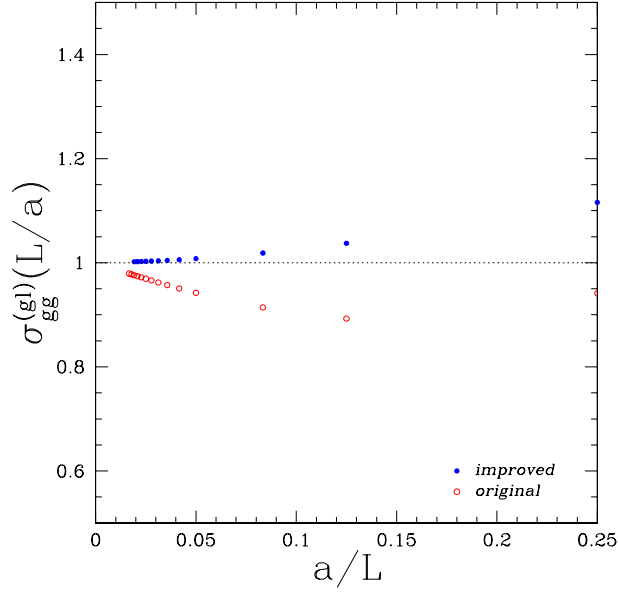


Fig. 13. Continuum approach of $[Z_{gg}^{(1)}]^{(gl)}$. Empty dots represent the original data, while the filled ones result from the cleaning procedure.

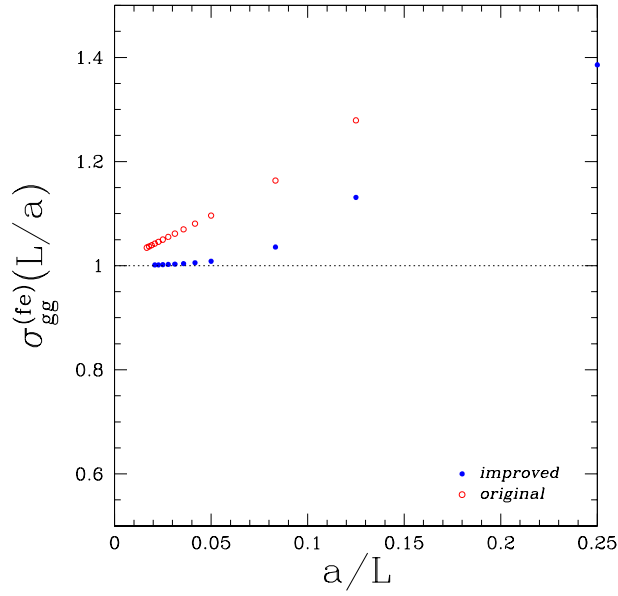


Fig. 14. Continuum approach of $[Z_{gg}^{(1)}]^{(fe)}$. Empty dots represent the original data, while the filled ones result from the cleaning procedure.

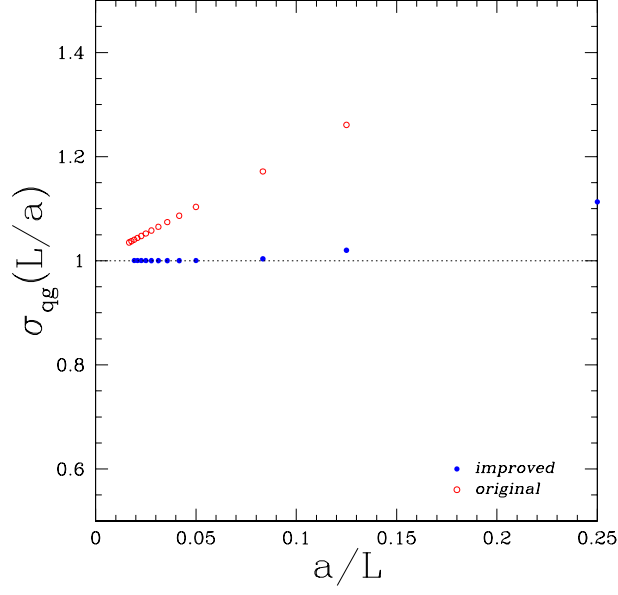


Fig. 15. Continuum approach of $Z_{qg}^{(1)}$. Empty dots represent the original data, while the filled ones result from the cleaning procedure.

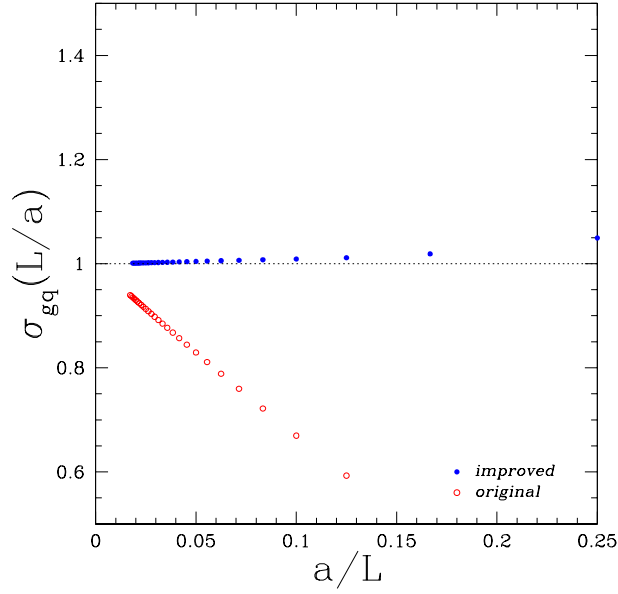


Fig. 16. Continuum approach of $Z_{gq}^{(1)}$. Empty dots represent the original data, while the filled ones result from the cleaning procedure.